

UCLA

UCLA Previously Published Works

Title

Resonant and Selective Excitation of Photocatalytically Active Defect Sites in TiO₂

Permalink

<https://escholarship.org/uc/item/40x7t0h9>

Journal

ACS Applied Materials & Interfaces, 11(10)

ISSN

1944-8244

Authors

Hou, Bingya
Shen, Lang
Shi, Haotian
[et al.](#)

Publication Date

2019-03-13

DOI

10.1021/acsami.8b12621

Peer reviewed

Resonant and Selective Excitation of Photocatalytically Active Defect Sites in TiO₂

Bingya Hou¹, Lang Shen², Haotian Shi³, Jihan Chen¹, Bofan Zhao¹, Kun Li⁵, Yi Wang³, Guozhen Shen⁶, Mai-Anh Ha⁷, Fanxi, Liu⁸, Anastassia N. Alexandrova^{7,9}, Wei Hsuan Hung¹⁰, Jahan Dawlaty³, Phillip Christopher⁵, and Stephen Cronin^{1,3,4}

¹Ming Hsieh Department of Electrical Engineering, ²Mork Family Department of Chemical Engineering and Materials Science, ³Department of Chemistry, ⁴Department of Physics and Astronomy, University of Southern California, Los Angeles, CA 90089, USA

⁵Department of Chemical Engineering, University of California, Santa Barbara, Santa Barbara, CA 93106-5080, USA

⁶State Key Laboratory for Superlattices and Microstructures, Institute of Semiconductors, Chinese Academy of Science, Beijing, 100083, P.R. China

⁷Department of Chemistry and Biochemistry, California NanoSystems Institute, University of California, Los Angeles, Los Angeles, CA 90025, USA

⁸Collaborative Innovation Center for Information Technology in Biological and Medical Physics, and College of Science, Zhejiang University of Technology, Hangzhou, 310023, P.R. China

⁹Materials Sciences Division, Lawrence National Laboratory, Berkeley, CA 94720, USA

¹⁰Department of Materials Science and Engineering, Feng Chia University, Taichung 407, Taiwan, 40724

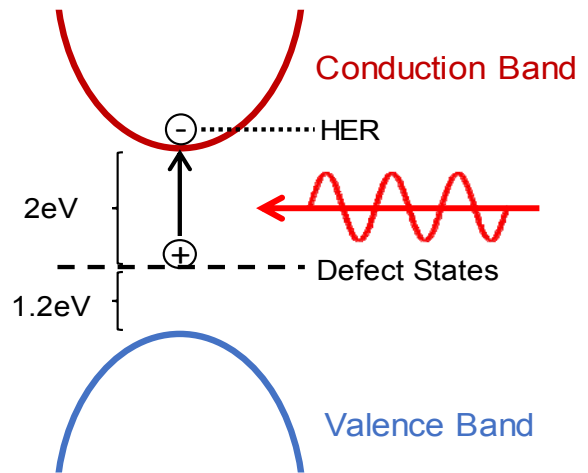
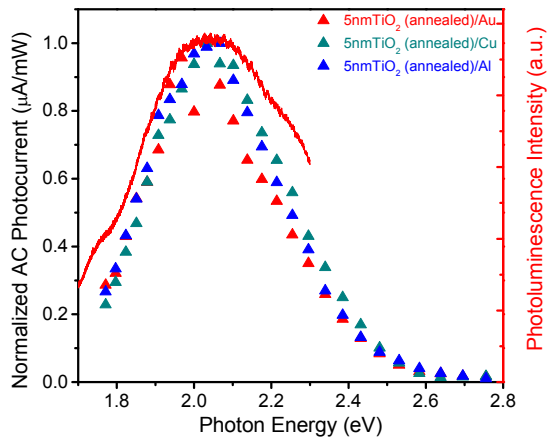
Abstract

It has been known for several decades that defects are largely responsible for the catalytically active sites on metal and semiconductor surfaces. However, it is difficult to directly probe these active sites because the defects associated with them are often relatively rare with respect to the stoichiometric crystalline surface. In the work presented here, we demonstrate a method to selectively probe defect-mediated photocatalysis, through differential AC photocurrent (PC) measurements. In this approach, electrons are photoexcited from the valence band to a relatively narrow distribution of sub-bandgap states in the TiO_2 , and then subsequently to the ions in solution. Because of their limited number, these defect states fill up quickly resulting in Pauli blocking, and are thereby undetectable under DC or CW excitation. In the method demonstrated here, the incident light is modulated with an optical chopper while the photocurrent is measured with a lock-in amplifier. Thin (5nm) films of TiO_2 deposited by atomic layer deposition (ALD) on various metal films, including Au, Cu, and Al, exhibit the same wavelength-dependent photocurrent spectra, with a broad peak centered around 2.0eV corresponding to the band-to-defect transition associated with the hydrogen evolution reaction (HER). While the UV-vis absorption spectra of these films show no features at 2.0eV, photoluminescence (PL) spectra of these photoelectrodes show a similar wavelength dependence with a peak around 2.0eV, corresponding to the sub-band gap emission associated with these defect sites. As a control, alumina (Al_2O_3) films exhibit no PL or PC over the visible wavelength range. The AC photocurrent plotted as a function of electrode potential, shows a peak around -0.4 to -0.1V vs. NHE, as the monoenergetic defect states are tuned through a resonance with the HER potential. This approach enables the direct photo-excitation of catalytically active defect sites to be studied selectively without the interference of the continuum interband transitions or

the effects of Pauli blocking, which is limited by the slow turnover time of the catalytically active sites, typically on the order of 1 μ sec. We believe this general approach provides an important new way to study the role of defects in catalysis in an area where selective spectroscopic studies of these are few.

Keywords: titania, titanium dioxide, resonate, photocatalysis, active site, catalysis

TOC Figure



Introduction

Defects in TiO₂ have been studied extensively, providing an important mechanism in photocatalytic energy conversion. In particular, oxygen vacancies (i.e., Ti³⁺ states) have been linked to catalytically active sites, particular in the water splitting and CO₂ reduction reactions systems.¹ TiO₂ films deposited by atomic layer deposition (ALD) are also known to have a high concentration of defects and, hence, show enhanced water splitting and CO₂ reduction efficiencies.²⁻⁵ Qiu et al. have quantified these O-vacancies (i.e., Ti³⁺ states) in ALD-deposited TiO₂ films using X-ray photoemission spectroscopy (XPS), and they have correlated these vacancies with the photocatalytic activity of TiO₂ films for both water splitting and CO₂ reduction reactions.^{2,4} Density functional theory calculations performed by Alexandrova's group have provided an atomistic picture of this enhancement mechanism, which show that both H₂O and CO₂ molecules bind stably to these non-stoichiometric Ti³⁺ states.^{3,6} Furthermore, when they allow their calculations to relax to their quantum mechanical ground state, they observe a spontaneous transfer of one electron creating CO₂⁻. In these DFT calculations, this CO₂⁻ species is bent and represents a high barrier intermediate species in this difficult reaction system.

In addition to oxygen vacancies, nitrogen defects can be created in TiO₂ by annealing in NH₃ gas, resulting in substantial sub-band gap absorption.⁷⁻⁹ This is a well-studied system in which the N-defect concentration can be controlled up to several percent by varying the annealing temperature. Extensive surface science studies of N-doping have been performed in the research groups of Rodriguez¹⁰ and Yates.¹¹⁻¹³ Doping of metal oxides by ion implantation, followed by calcinations in oxygen, has also been studied extensively as a means of dramatically increasing in the photocatalytic activity in the visible wavelength range.¹⁴⁻²³ Among the elements

studied, V, Cr, Mn, Fe, and Ni were found to increase the photocatalytic activity of TiO₂ in the visible range substantially.²⁴

In the work presented here, an AC lock-in measurement technique is employed to study photocatalysis, revealing the behavior of sub-band gap states, that are resonant in both wavelength and electrode potential, and give rise to a substantial increase in photocurrent in the hydrogen evolution reaction (HER) process. In order to further characterize these sub-band gap states, we collect photoluminescence (PL) spectra, which provide an independent measure of the energetics of these important sub-band gap states. UV-Vis spectra are also obtained in order to provide a complete picture of the band edge and sub-band gap absorption in the TiO₂ thin film with and without annealing.

Photoelectrodes were fabricated by depositing 100 nm thick films of Au, Cu and Al on glass substrates using electron beam deposition. A 5 nm TiO₂ film was then deposited by ALD at 250°C using TDMAT as the Ti source and water vapor as the O source. The base flow rate during deposition was 20 sccm. The TiO₂ thickness was established by ellipsometry for a 5 nm film, which corresponds to 100 ALD cycles. The TiO₂/Au films were annealed in a quartz tube furnace at 450°C for 30 min while O₂ gas was flowing. The TiO₂/Cu and TiO₂/Al films were annealed in a quartz tube furnace at 450°C for 30 min while argon gas was flowing. UV-vis absorption spectra of a 10nm thick TiO₂ film taken before and after annealing are plotted in Figure S1 of the supplemental information. Figure 1(a) shows an illustration of the sample geometry, in which an insulated copper wire was attached to the TiO₂/metal electrode using silver paint and the whole sample, excluding the top surface, was encased in epoxy to insulate it from the electrolytic solution. Photoelectrochemical measurements were performed using a three terminal potentiostat (Gamry, Inc.), as illustrated in Figure 1(b). For the HER, a Ag/AgCl reference electrode was used and a Pt wire was used as the counter electrode. The electrodes were immersed in a pH=7, Na₂SO₄ solution. We used an AC lock-in technique, which enables us

to detect the relatively small photocurrents (μA) produced by just 5nm of wide-band gap semiconductor material. In order to vary the wavelength of the incident light, a 1000W xenon lamp was used in conjunction with a monochromator to produce monochromatic light throughout the visible wavelength range. The power reaching the sample surface was 2-3mW. Here, the light was filling the entire sample area. The incident light was chopped at frequency ω_{chopper} , which was 200 Hz in our case. The chopper controller (Stanford Research Systems, Inc., Model SR540) was connected to the “REF IN” terminal of the lock-in amplifier (Standard Research Systems, Model SRS830 DSP), in order to synchronize the lock-in amplifier with the light modulation. The AC voltage signal from the auxiliary current monitor terminal of the potentiostat was used as the input signal of the lock-in amplifier in order to collect the AC photocurrent generated by the $\text{TiO}_2/\text{metal}$ films.

Figure 2 shows the AC and DC photocurrents plotted as a function of the reference potential for the HER for 5nm TiO_2 deposited on Au and Cu. Here, we observe a peak in the AC photocurrent around -0.13V vs. NHE corresponding to the conditions under which we tune the potential of the charge associated with the resonantly-excited defect states through the redox potential of the HER half-reaction. This is considerably shifted from the DC onset potential of -0.3V vs. NHE. For the TiO_2/Cu electrode, the peak in AC photocurrent is observed at -0.4V vs. NHE, which is also substantially shifted with respect to the DC onset potential of -0.6V vs. NHE.

Figure S4 shows the light intensity dependence of the AC photocurrent from a TiO_2/Au sample obtained for both reduction and oxidation reactions under 532nm illumination. Here, we observe a linear response to the light intensity, as expected. This result indicates that we are successfully converting photons to hot carriers under optical excitation.²⁵

Figure 3(a) shows the normalized AC photocurrent spectra of 5nm TiO₂ deposited on Au, Cu, and Al. Here, a clear peak can be seen around 2eV, which is well below the 3.2eV bandgap of this material. This feature at 2eV corresponds to the photo-excitation of the sub-band gap defect states that serve as catalytically-active sites for the HER, as illustrated in Figure 3(b). Further evidence for this defect state is provided by the PL spectrum, also plotted in Figure 3(a), which also exhibits a peak centered around 2.0eV. Interestingly, no such feature can be seen in the UV-vis absorption spectra at 2.0eV. Figure S1 of the supplemental information shows the UV-vis absorption spectra of both annealed and unannealed TiO₂ films. Here, both spectra show moderate sub-band gap absorption that is monotonically decreasing with wavelength. However, no specific feature is present in these UV-vis spectra at 2.0eV. This indicates that, while there are likely many different types of defect states throughout the band gap, there is a specific defect located at 1.2eV above the valence band edge that is catalytically active for the hydrogen evolution reaction.

Ultraviolet photoemission spectroscopy (UPS) is a common tool to study conduction and valence band structure of materials.^{26, 27} The valence band spectrum of an oxygen-annealed 5nm TiO₂ film was obtained by UPS at 21.2eV photon energy. The linear plot, Figure 4(a), shows the position of valence band edge. The valence band edge is 3.2eV below the Fermi energy, which is pinned at the conduction band edge. After annealing, a peak at approximately 2eV below the conduction band edge was observed in the log plot, as shown in Figure 4(b), which agrees with the peak position of photocurrent spectra.

Figure S3 shows an X-ray photoemission spectroscopy (XPS) spectrum of a 5nm TiO₂ film deposited on a Au film by atomic layer deposition. In addition to the main Ti⁴⁺ peaks, which

correspond to stoichiometric TiO_2 , we observe a small shoulder peak corresponding to Ti^{3+} states (i.e., oxygen-vacancies), as reported previously by Qiu et al.²⁸

High resolution cross-sectional transmission electron microscope (TEM) images were taken of 5nm and 25nm thick TiO_2 films deposited on Au films. Figure S2(c) shows amorphous TiO_2 material, as expected. This material is non-stoichiometric and contains a high density of oxygen vacancies, as evidenced by the UPS and XPS spectra described above. In contrast, Figure S2(d) shows crystalline material. Qiu et al. have also demonstrated that above 10nm, TiO_2 films become crystalline.²⁹ These thicker TiO_2 films are crystalline and have poor charge transfer characteristics due to their insulating nature. Thus, we are more interested in thin and amorphous TiO_2 films.

Plane-wave density functional theory (PW-DFT) calculations were performed on defective (101) anatase in order to extract formation energies and spectral analyses of oxygen vacancies. A single oxygen vacancy results in the presence of 2 excess electrons that may localize on neighboring Ti atoms. Experimentally, spectral signatures were found $\sim 2\text{eV}$ from the Fermi energy. Due to the over-delocalization of electrons in DFT, we introduced a strong Hubbard U parameter of 4.0eV into our calculations in order to recover a theoretical band gap is $\sim 2.2\text{eV}$. Utilizing Bader charge analysis, we were able to determine the localization of electrons on surface Ti sites. For surface oxygen vacancies V_{O1} and V_{O2} , electrons localized on neighboring Ti atoms $\sim 1.9\text{\AA}$ from the vacancy site. For surface oxygen vacancy V_{O3} , the two electrons localized on Ti atoms farther away from the vacancy site, one on a Ti atom $\sim 1.9\text{\AA}$ and the other on a Ti atom $\sim 3.7\text{\AA}$ from the vacancy site. The ramifications of this may be found in the theoretical density of states shown in Figure S7(b). In comparison to V_{O1-O2} , V_{O3} 's spectral signatures of the localized electrons are shifted farther away from the Fermi energy. We

hypothesize that at the deeper oxygen vacancy sites, the spectral signatures of the localized electrons also shift farther away from the Fermi energy. However, the small theoretical band gap of $\sim 2.2\text{eV}$ may obscure these spectral signatures and so, we focus only on V_{O1-O3} . Based on these DFT calculations, it seems that the specific catalytically active defect sites that we observe in our photoelectrochemical measurements actually correspond to sub-surface defects. While these results provide qualitative agreement with our experimental results (i.e., sub-band gap states giving rise to visible light absorption, it is not possible to assign a specific atomic defect to our observation, and it is likely that a large collective ensemble of these defects contribute to the broad spectral distribution observed experimentally.

In our previous work, similar structures consisting of Au films with and without TiO_2 coatings were investigated.³⁰ For the bare metal electrodes, the mechanism of photocatalysis was attributed to hot electrons photoexcited in the metal. The mechanism of photocurrent generation in TiO_2 -coated Au electrodes was attributed to hot electron injected by the metal film because of our inability to detect these defect states in the UV-vis absorption process. However, these defect states are somewhat elusive because of the Pauli blocking associated with their finite density and slow turnover time, and we now have a better understanding of this system. It should be noted that the photoexcited charge generated at these O-vacancy defect sites is bound to the defect site and is not free to propagate throughout the TiO_2 crystal.

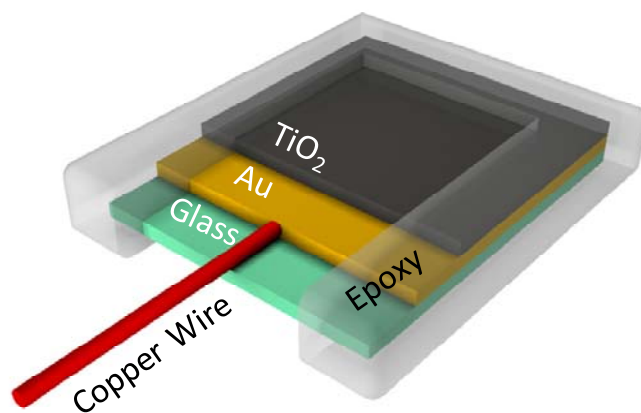
In conclusion, we have demonstrated a method to selectively probe defect-mediated photocatalysis through differential AC photocurrent measurements. Here, we drive the photoexcitation of electrons (or holes) from the valence band to relatively narrow distribution of sub-band gap states, and then to the ions in solution. Because of their limited number, these defect states fill up quickly resulting in Pauli blocking and are undetectable under DC or CW

conditions. In the method demonstrated here, the incident light is modulated with an optical chopper and the photocurrent is measured with a lock-in amplifier. Thin (5nm) films of TiO₂ deposited on different metals (Au, Cu, and Al) using ALD exhibit the same wavelength-dependent photocurrent spectra, with a broad peak centered around 2.0eV. PL spectra also show a peak at 2.0eV, corresponding to the sub-band gap emission associated with these defect sites. In addition, the AC photocurrent shows a peak around -0.4 to -0.1V vs. NHE, as the monoenergetic defect states are tuned through a resonance with the HER potential. This approach enables the photoexcitation of catalytically active defect sites to be studied selectively without the interference from the continuum of interband transitions or the effects of Pauli blocking, which is quite pronounced because of the slow turnover time (~1μsec) of the catalytically active sites.

Acknowledgements: This research was supported by Air Force Office of Scientific Research (AFOSR) Grant No. FA9550-15-1-0184 (B.H.), National Science Foundation (NSF) Award No. CBET-1512505 (L.S. and J.C.), and Army Research Office (ARO) Award No. W911NF-14-1-0228 (H.S.).

Figures

(a)



(b)

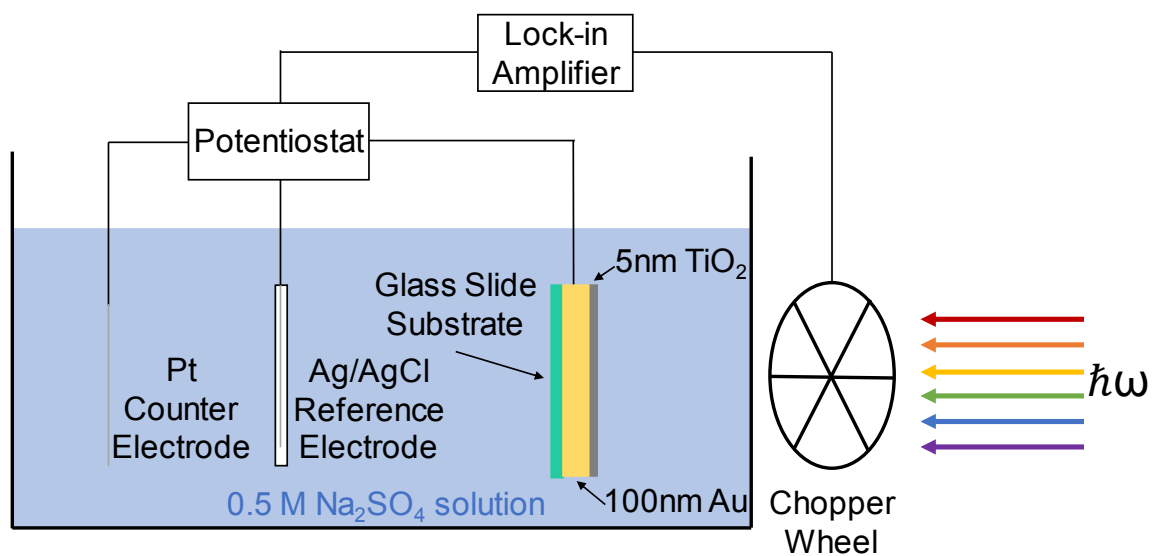


Figure 1. (a) Diagram illustrating the sample configuration. (b) Schematic diagram of the three-terminal photoelectrochemical setup with the modulated light and AC lock-in amplifier.

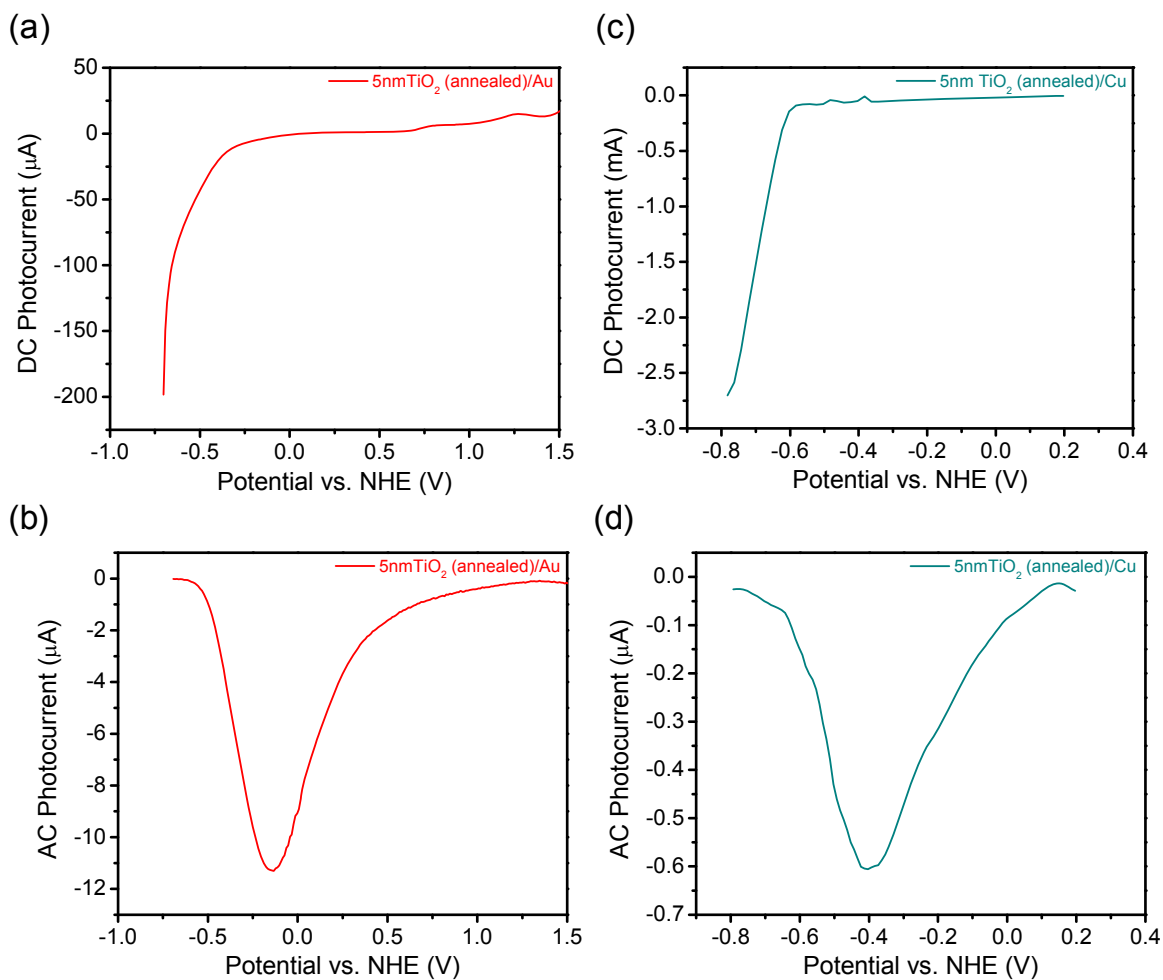


Figure 2. DC (a, c) and AC (b, d) photocurrent plotted as a function of the reference potential for the hydrogen evolution reaction (HER) for (a, b) 5nm annealed TiO₂ deposited on Au under 532nm illumination. (c, d) 5nm annealed TiO₂ deposited on Cu under 532nm illumination.

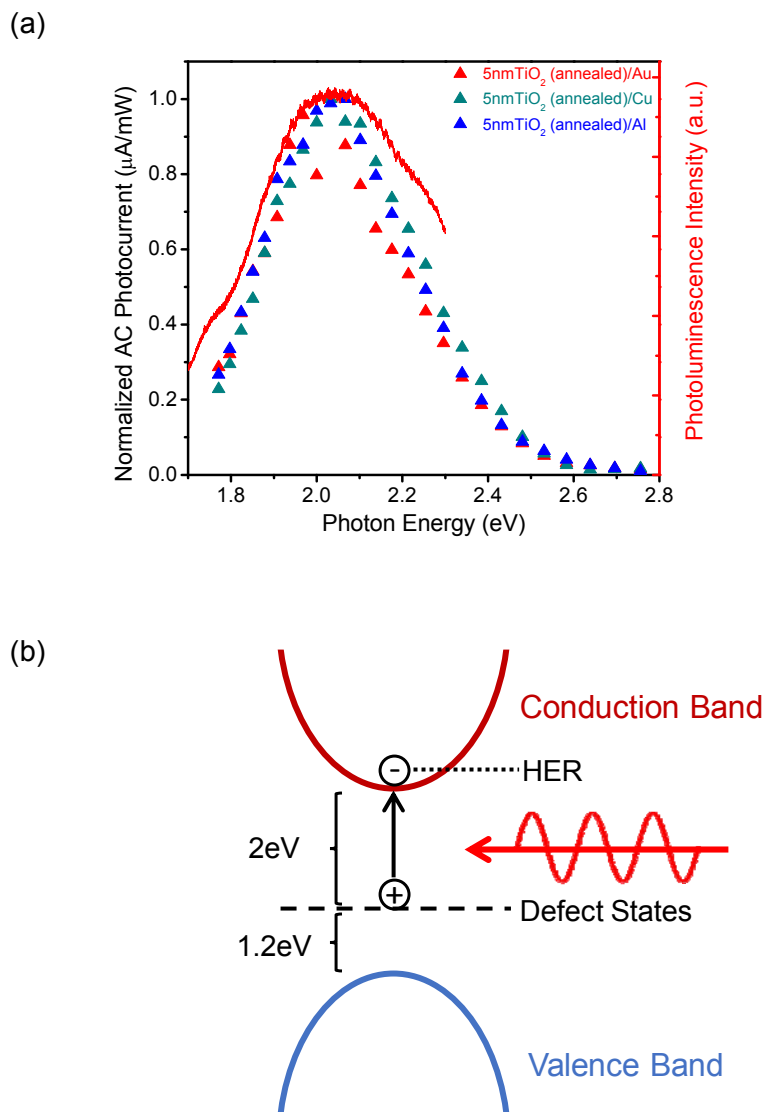


Figure 3. (a) Normalized AC photocurrent spectra of 5nm TiO₂ deposited on Au, Cu, and Al films and corresponding photoluminescence spectrum of 5nm thick annealed TiO₂ deposited on a Au film. (b) Energy band diagram of the photoexcitation mechanism of defect-mediated photocatalysis.

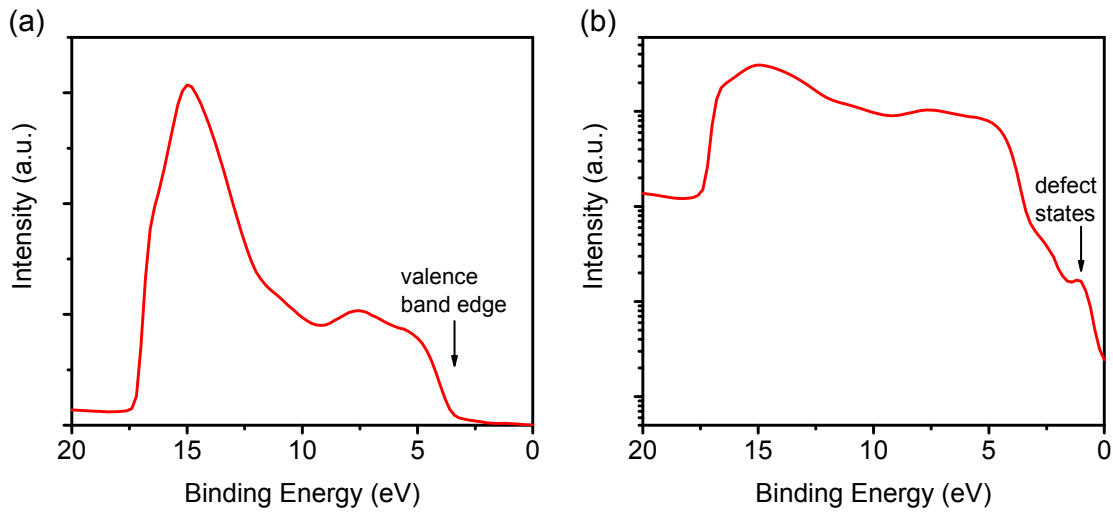


Figure 4. Valence band spectra of a 5nm TiO₂ film obtained by UPS at 21.2eV photon energy plotted on (a) linear and (b) log scales.

ASSOCIATE CONTENT

Supporting Information available:

UV-Vis absorption spectra, High resolution TEM images, XPS spectrum, Frequency dependence of AC photocurrent, Light intensity dependence of AC photocurrent, PL spectra, Transient absorption spectra, Density functional theory calculation, AC photocurrent for 5nm and 25nm annealed TiO₂.

References

1. Lu, G., Amy Linsebigler, and John T. Yates Jr., Ti^{3+} Defect Sites on $\text{TiO}_2(110)$: Production and Chemical Detection of Active Sites. *The Journal of Physical Chemistry C* 1994, 98, 11733-11738.
2. Qiu, J.; Zeng, G. T.; Ge, M. Y.; Arab, S.; Mecklenburg, M.; Hou, B. Y.; Shen, C. F.; Benderskii, A. V.; Cronin, S. B., Correlation of Ti^{3+} states with Photocatalytic Enhancement in TiO_2 -passivated p-GaAs. *Journal of Catalysis* 2016, 337, 133-137.
3. Qiu, J.; Zeng, G. T.; Ha, M. A.; Hou, B. Y.; Mecklenburg, M.; Shi, H. T.; Alexandrova, A. N.; Cronin, S. B., Microscopic Study of Atomic Layer Deposition of TiO_2 on GaAs and Its Photocatalytic Application. *Chemistry of Materials* 2015, 27, 7977-7981.
4. Zeng, G. T.; Qiu, J.; Hou, B. Y.; Shi, H. T.; Lin, Y. J.; Hettick, M.; Javey, A.; Cronin, S. B., Enhanced Photocatalytic Reduction of CO_2 to CO through TiO_2 Passivation of InP in Ionic Liquids. *Chemistry-a European Journal* 2015, 21, 13502.
5. Zeng, G.; Qiu, J.; Pavaskar, P.; Li, Z.; Cronin, S. B., CO_2 Reduction to Methanol on TiO_2 -Passivated GaP Photocatalysts. *ACS Catalysis* 2014, 4, 3512.
6. Qiu, J.; Zeng, G.; Ha, M. A.; Ge, M.; Lin, Y.; Hettick, M.; Hou, B.; Alexandrova, A. N.; Javey, A.; Cronin, S. B., Artificial Photosynthesis on TiO_2 -Passivated InP Nanopillars. *Nano letters* 2015, 15, 6177-81.
7. Linic, S.; Christopher, P.; Ingram, D. B., Plasmonic-Metal Nanostructures for Efficient Conversion of Solar to Chemical Energy. *Nature Materials* 2011, 10, 911-921.
8. Irie, H.; Watanabe, Y.; Hashimoto, K., Nitrogen-Concentration Dependence on Photocatalytic Activity of $\text{TiO}_{2-x}\text{N}_x$ Powders. *Journal of Physical Chemistry B* 2003, 107, 5483-5486.
9. Asahi, R.; Morikawa, T.; Ohwaki, T.; Aoki, K.; Taga, Y., Visible-Light Photocatalysis in Nitrogen-Doped Titanium Oxides. *Science* 2001, 293, 269-271.
10. Nambu, A.; Graciani, J.; Rodriguez, J. A.; Wu, Q.; Fujita, E.; Sanz, J. F., N Doping of $\text{TiO}_2(110)$: Photoemission and Density-Functional Studies. *J Chem Phys* 2006, 125, 8.
11. Thompson, T. L.; Yates, J. T., Control of a Surface Photochemical Process by Fractal Electron Transport across the Surface: O^{-2} Photodesorption from $\text{TiO}_2(110)$. *J Phys Chem B* 2006, 110, 7431-7435.
12. Diwald, O.; Thompson, T. L.; Zubkov, T.; Goralski, E. G.; Walck, S. D.; Yates, J. T., Photochemical Activity of Nitrogen-Doped Rutile $\text{TiO}_2(111)$ in Visible Light. *J Phys Chem B* 2004, 108, 6004-6008.
13. Diwald, O.; Thompson, T. L.; Goralski, E. G.; Walck, S. D.; Yates, J. T., The effect of nitrogen ion implantation on the photoactivity of TiO_2 rutile single crystals. *J Phys Chem B* 2004, 108, 52-57.
14. Anpo, M.; Dohshi, S.; Kitano, M.; Hu, Y.; Takeuchi, M.; Matsuoka, M., The Preparation and Characterization of Highly Efficient Titanium Oxide-Based Photofunctional Materials. *Annual Review of Materials Research* 2005, 35, 1-27.
15. Yamashita, H.; Harada, M.; Misaka, J.; Takeuchi, M.; Neppolian, B.; Anpo, M., Photocatalytic Degradation of Organic Compounds Diluted in Water Using Visible Light-Responsive Metal Ion-Implanted TiO_2 Catalysts: Fe Ion-Implanted TiO_2 . *Catalysis Today* 2003, 84, 191-196.
16. Yamashita, H.; Harada, M.; Misaka, J.; Takeuchi, M.; Ikeue, K.; Anpo, M., Degradation of Propanol Diluted in Water Under Visible Light Irradiation Using Metal Ion-Implanted

Titanium Dioxide Photocatalysts. *Journal of Photochemistry and Photobiology A-Chemistry* 2002, 148, 257-261.

17. Takeuchi, M.; Yamashita, H.; Matsuoka, M.; Anpo, M.; Hirao, T.; Itoh, N.; Iwamoto, N., Photocatalytic Decomposition of NO on Titanium Oxide Thin Film Photocatalysts Prepared by an Ionized Cluster Beam Technique. *Catal Lett* 2000, 66, 185-187.

18. Yamashita, H.; Harada, M.; Misaka, J.; Takeuchi, M.; Ichihashi, Y.; Goto, F.; Ishida, M.; Sasaki, T.; Anpo, M., Application of Ion Beam Techniques for Preparation of Metal Ion-Implanted TiO₂ Thin Film Photocatalyst Available Under Visible Light Irradiation: Metal Ion-Implantation and Ionized Cluster Beam Method. *Journal of Synchrotron Radiation* 2001, 8, 569-571.

19. Anpo, M., Utilization of TiO₂ Photocatalysts in Green Chemistry. *Pure and Applied Chemistry* 2000, 72, 1265-1270.

20. Anpo, M., Use of Visible Light. Second-Generation Titanium Oxide Photocatalysts Prepared by the Application of an Advanced Metal Ion-Implantation Method. *Pure and Applied Chemistry* 2000, 72, 1787-1792.

21. Iino, K.; Kitano, M.; Takeuchi, M.; Matsuoka, M.; Anpo, M., Design and Development of Second-Generation Titanium Oxide Photocatalyst Materials Operating Under Visible Light Irradiation by Applying Advanced Ion-Engineering Techniques. *Current and Applied Physics* 2006, 6, 982-986.

22. Takeuchi, M.; Yamashita, H.; Matsuoka, M.; Anpo, M.; Hirao, T.; Itoh, N.; Iwamoto, N., Photocatalytic Decomposition of NO Under Visible Light Irradiation on the Cr-Ion-Implanted TiO₂ Thin Film Photocatalyst. *Catal Lett* 2000, 67, 135-137.

23. Anpo, M.; Che, M., Applications of Photoluminescence Techniques to the Characterization of Solid Surfaces in Relation to Adsorption, Catalysis, and Photocatalysis. *Advances in Catalysis* 2000, 44, 119-257.

24. Choi, W. Y.; Termin, A.; Hoffmann, M. R., The Role of Metal-Ion Dopants in Quantum-Sized TiO₂ - Correlation between Photoreactivity and Charge-Carrier Recombination Dynamics. *J Phys Chem-Us* 1994, 98, 13669-13679.

25. Mukherjee, S.; Zhou, L.; Goodman, A. M.; Large, N.; Ayala-Orozco, C.; Zhang, Y.; Nordlander, P.; Halas, N. J., Hot-Electron-Induced Dissociation of H₂ on Gold Nanoparticles Supported on SiO₂. *Journal of the American Chemical Society* 2014, 136, 64-7.

26. Fleming, L.; Fulton, C.; Lucovsky, G.; Rowe, J.; Ulrich, M.; Lüning, J., Local Bonding Analysis of the Valence and Conduction Band Features of TiO₂. *Journal of Applied Physics* 2007, 102, 033707.

27. Tao, J.; Luttrell, T.; Batzill, M., A Two-Dimensional Phase of TiO₂ with a Reduced Bandgap. *Nature chemistry* 2011, 3, 296.

28. Qiu, J.; Zeng, G.; Ge, M.; Arab, S.; Mecklenburg, M.; Hou, B.; Shen, C.; Benderskii, A. V.; Cronin, S. B., Correlation of Ti³⁺ States with Photocatalytic Enhancement in TiO₂-Passivated p-GaAs. *Journal of Catalysis* 2016, 337, 133-137.

29. Qiu, J.; Zeng, G.; Ha, M.-A.; Hou, B.; Mecklenburg, M.; Shi, H.; Alexandrova, A. N.; Cronin, S. B., Microscopic Study of Atomic Layer Deposition of TiO₂ on GaAs and Its Photocatalytic Application. *Chemistry of Materials* 2015, 27, 7977-7981.

30. Hou, B.; Shen, L.; Shi, H.; Kapadia, R.; Cronin, S. B., Hot Electron-Driven Photocatalytic Water Splitting. *Physical chemistry chemical physics : PCCP* 2017, 19, 2877-2881.